Modeling scattering of cross-well seismic waves using Radiative Transfer Theory

Josimar A. Da Silva Jr, Oleg V. Poliannikov and Michael Fehler, Earth Resources Laboratory / M.I.T

SUMMARY

We model P and S-wave mean square envelopes in 2-D random media by solving the Radiative Transfer Theory (RTT) equation using a Monte Carlo (MC) particle based approach. Using a source frequency in the order of kilohertz, typical of cross-well seismic sources, we find good agreement with finite differences in both effective and forward scattering regimes. We show that MC simulations is a much faster way of modeling scattering attenuation, compared to finite differences, and therefore is a suitable tool to characterize the medium heterogeneities associated, for example, with highly fracture reservoirs.

INTRODUCTION

The propagation of seismic waves through heterogeneous media results in multiple scattering of P and S-waves. Contrarily to intrinsic attenuation, scattering attenuation redistributes the wave energy throughout the seismogram. Previous work in seismology have shown that P and S-wave coda are the result of scattering attenuation (Aki and Chouet, 1975) and since then different approaches have been proposed to model the P and S-wave envelopes as a function of the medium scattering properties.

A popular model used in global seismology to simulate seismogram envelope is based on the Radiative Transfer Theory (RTT) (Wu, 1985), which describes energy transport through a scattering medium neglecting phase information. Initially derived to describe scattering of light in the atmosphere (Chandrasekhar, 1950) , the RTT equation was later derived from the elastic wave equation (Ryzhik et al., 1996). Analytical solutions to the RTT equation exist for the case of isotropic scattering in both acoustic (Zeng et al., 1991; Paasschens, 1997) and elastic cases (Zeng, 1993). For the case of anisotropic scattering, the RTT equation has been solved numerically using Monte Carlo (MC) simulations and the Born scattering coefficients (Przybilla et al., 2006; Przybilla and Korn, 2008). Comparison with finite difference (FD) simulations for low frequencies (2 Hz) has shown good agreement between MC envelopes and FD from the P-wave onset to the later S-wave coda (Wegler et al., 2006; Przybilla et al., 2006).

Previous works using Monte Carlo simulations to solve the RTT equation have focused mostly in the strong forward scattering regime aiming at investigating the scattering properties of the crust (Przybilla et al., 2009; Gaebler et al., 2015) and upper mantle (Shearer and Earle, 2004) using regional and global earthquakes, respectively. In this paper we show that solving the RTT equation using Monte Carlo simulations is also an effective tool to model P and S-wave envelopes using high frequency waves and therefore can be used effectively to characterize a medium heterogeneities associated, for example, with fractured reservoirs in the context of exploration seismology.

We consider the context of cross-well seismic monitoring, with typical frequencies in the order of kilohertz (Daley et al., 2007). We use finite difference (FD) simulation to generate synthetic seismograms in a randomly heterogeneous medium, with varying sizes of heterogeneities. We then generate mean square envelopes (MS) using Monte Carlo simulations for the same set of medium parameters. We find good agreement between the two methods and show that MC simulations is much faster than FD.

STATISTICAL MODELING OF SCATTERERS

In solving for the wavefield in a heterogeneous medium using FD, we use a velocity model in which velocity perturbations are distributed spatially according to a statistical model with predefined auto-correlation function (ACF).

The wave velocity field V is considered to be the sum of a mean velocity V_0 and a perturbed velocity δV which depends on the location $\mathbf{x}$ (Sato et al., 2012):

$$V(\mathbf{x}) = V_0 + \delta V(\mathbf{x}) = V_0[1+\xi(\mathbf{x})] \tag{1}$$

where $\xi(\mathbf{x}) \equiv \delta V(\mathbf{x})/V_0$ is the fractional velocity fluctuation that will be represented by a random function of coordinate $\mathbf{x}$. A sample $\xi(\mathbf{x})$ of the enseble of random media $\{\xi\}$ can be obtained in space by Fourier transform where the amplitude spectrum is given by using $\sqrt{P(\mathbf{m})}$, where $P(\mathbf{m})$ is the power spectral density function (PSDF). Different samples $\xi(\mathbf{x})$ can be obtained by randomizing the phase spectra (Sato et al., 2012).

There are many different types of PSDFs that are used to describe subsurface heterogeneites with a variety of scale sizes. The fact that the earth's materials have heterogeneities in all scales favors the usage of PSDFs with self-affine properties (Klimes, 2002; Sato et al., 2012). Here we will focus on a PSDF given by a von Karman ACF, which has a power law decay and therefore represents heterogeneities in a broad range scales. In 2-D its PSDFs is given by (Przybilla et al., 2006):

$$P(m) = \frac{4\pi\Gamma(\kappa+1)\varepsilon^2 a^2}{\Gamma(\kappa)(1+a^2m^2)^{\kappa+1}} \tag{2}$$

Where a is the correlation distance, ε is the fractional fluctuation, m is the wavenumber, Γ is the gamma function and κ is a parameter that controls the power law decay of the von Karman PSDF. Using well logs from the German Continental Deep Drilling project (KTB), Wu et al. (1994) found a power law decay for the crust heterogeneities. Examples of other applications of the von Karman PSDF to describe geological features can be found in Klimes (2002) and Przybilla et al. (2009).

Modeling scattering attenuation using Monte Carlo simulations

MODEL GEOMETRY

We are interested in characterizing the scattering properties of a medium. We choose to design an experiment corresponding to a cross-well seismic geometry, with source frequency equal to 1000 Hz (Daley et al., 2007). The short wavelength generated by cross well seismic sources provides high resolution images of the sampled media (Daley et al., 2007). Here we will assume that the source used in cross-well seismic experiments generates only P waves. Figure 1 shows the model geometry where an explosive source is at the center of the model and receivers are located with a minimum offset of 50 m. The model parameters are summarized in table 1. We then use both FD and the RTT to model the mean square envelopes that result from the propagation through the random velocity perturbations as shown in figure 1.

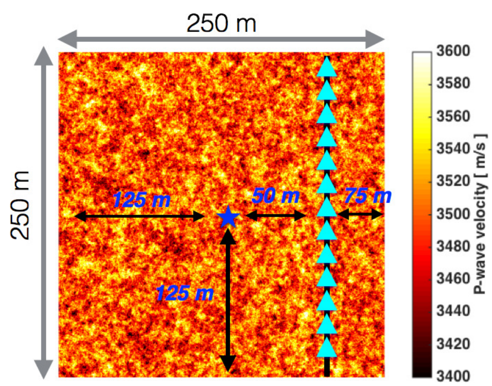

Figure 1: Model geometry with source (blue star) and receiver (cyan triangles) locations superimposed on a heterogeneous P-wave velocity generated using a von Karman PSDF.

Modeling Parameters		
$V_p = 3500$ (m/s)	$\gamma_0 = \frac{V_P}{V_S} = \sqrt{3}$	$\nu = 0.6518$
$\lambda_P = 3.5$ m	$\lambda_S = 2.02$ m	$f = 1000$ Hz
offsets: 50 m, 60 m 70 m and 80 m		

Table 1: Modeling parameters used to simulate P and S-wave mean square envelopes. The source and receiver locations are shown in figure 1. Here ν is the velocity density conversion factor.

ENVELOPE MODELING USING MONTE CARLO SIMULATIONS

The radiative transfer equation can be solved numerically using a Monte Carlo particle based aproach (Shearer and Earle, 2004; Przybilla et al., 2006; Przybilla and Korn, 2008). In this approach millions of particles are sprayed from the source and scattered through the heterogeneous medium according to probabilities given by the Born scattering coefficients. There are many advantages of this method: energy is conserved, single and multiple scattering are naturally included and intrinsic attenuation can be easily included for both P and S-waves.

Each particle taking off from the source will propagate through the medium with background P and S-wave velocities, if the particle is P or S, respectively, and scatter at a distance given by an exponential distribution as:

$$s_p = -l_p \ln\gamma \qquad s_s = -l_s \ln\gamma \tag{3}$$

With a uniformly distributed random number $\gamma \in (0,1]$. In equation 3, s_p, s_s, l_p and l_s are the distance for a scattering event to occur and the mean free paths for both P and S particles. The mean free paths are related to the total scattering coefficients as:

$$l_p = (g^0_{pp} + g^0_{ps})^{-1} \qquad l_s = (g^0_{ss} + g^0_{sp})^{-1} \tag{4}$$

Where $g^0_{PP}, g^0_{PS}, g^0_{SP}$ and g^0_{SS} are the total scattering coefficients for P and S waves given by averaging the single scattering coefficients ($g_{PP}, g_{PS}, g_{SP}, g_{SS}$) over the unit circle. Expressions for the scattering coefficients can be found in Przybilla et al. (2006) for the 2-D case and in Sato et al. (2012) for the 3-D case. All the scattering coefficients are given by similar expressions and can be written in the following simplified functional form (Przybilla et al., 2009):

$$g_{ij} = \frac{\varepsilon^2}{a} F(ak_s) \tag{5}$$

where i, j is P or S. The scattering coefficients are the product of the parameter combination ε^2/a and the functional F in which the heterogeneity correlation length a and the S-wave number $k_s = 2\pi/\lambda_s$ only occur as a product. The direction dependence of scattering is constroled by the parameter combination ak_s. If scattering occurs, then for $ak_s \ll 1$ waves are scattered mainly in the backward direction and $ak_s \gg 1$ waves are scattered mainly in the forward direction. For $ak_s \sim 1$, waves interact intensively with the medium and scattering is strong because the wavelength is on the order of the correlation length a of the medium. This regime is also known as effective scattering regime.

In Monte Carlo simulations the particles travels a distance to the next scatterer according to probabilities given by equation 3. Whe scattering occurs, the conversion between different phases is a Markov process where each state represents either P or S particles. The transition probability Π between state i and j, representing P and S particles, respectively, is given by (Przybilla et al., 2006):

$$\Pi(i \text{ to } j) = \frac{g^0_{ii}}{g^0_{ii} + g^0_{ij}}, \quad \Pi(i \text{ to } j) = 1 - \Pi \quad (j \text{ to } i) \tag{6}$$

At every scattering point a random number is used to decide weather phase conversion occurs or not. Figure 2 shows the total scattering coefficients as a function of the control parameter ak_s. Phase conversion occurs mainly in the effective scattering regime ($ak_s \approx 1$). Here we are interested in modeling P and S-wave envelopes for a cross-well seismic source, which we assume generates only P waves. Therefore it is expected that away from the effective scattering regime, (e.g $ak_s \gg 1$) there is almost no S-wave energy.

The scattering coefficients given in equation 5 are calculated for each type of random medium (Sato et al., 2012) used to estimate the angle that a particle will travel after scattering. Figure 3 show examples of scattering directions for different scattering regimes for a von Karman medium. When only P-to-P conversions occurs, such as the case of strong forward scattering regime ($ak_s \gg 1$), it is expected that scattering will occur mainly in the -10 to 10 degree direction, for example. For $ak \sim 3.1$ there is a wider range of possible angles. The scattering coefficients are converted to probabilities and then compared with a random number in order to decide the new scattering direction.

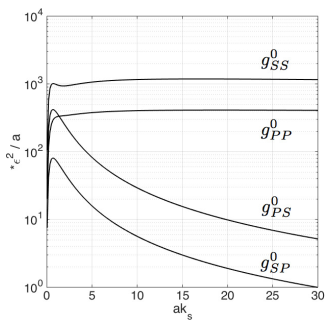

Figure 2: Total scattering coefficients as a function of control parameter ak_s for a von Karman medium. P-to-S conversions occur mainly in the effective scattering regime where $ak_s \sim 1$.

	l_p	l_s
$ak_s = 3.1$	45 m	24 m
$ak_s = 31$	5.6 m	2 m

Table 2: Medium parameters used in the Monte Carlo simulations for two scattering regimes. $ak_s = 3.1$ and $ak_s = 31$ corresponds to $a = 1$ m and $a = 10$ m respectively. l_p and l_s are the mean free paths for P and S-waves, respectively. For the von Karman media it was used $\kappa = 0.3$.

During the particle propagation through the geometry in figure 1 we allow particles to scatter until a maximum time $t_{max} = 0.06$ s. For an S-wave particle following a straight path, this corresponds to a distance $d \approx 120$ m, therefore particles with travel time larger than t_{max} are far from the receiver and do not generate a recorded signal.

For each receiver located at distance r from the source, we count the number of particles $N(r,t_i)$ that cross a circle of radius λ_P around the receiver in a small time step Δt, where λ_p is the P-wave wavelength. The energy density, which is proportional to the mean square envelope (MS), is then given by:

$$E(r,t_i) = \frac{N(r,t_i)}{N_0 A(r)} \quad (7)$$

Where N_0 is the total number of particles shot from the source, in our case taken to be $N_0 = 10^6$, and $A(r)$ is the area of the circle surrounding the receiver. Figure 4 shows examples of mean square envelopes for a von Karman medium for different offsets. Note the variation of the S-wave envelope amplitude with offset and the convergence, at larger lapse times, to a background value.

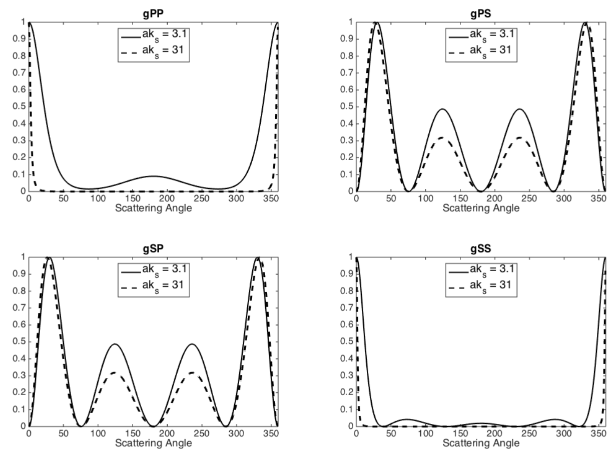

Figure 3: Normalized scattering coefficients as a function of the scattering angle (eq. 6 and 8) for effective scattering ($ak_s = 3.1$) and forward scattering regime ($ak_s = 31$). A von Karman PSDF with parameters given in tables 1 and 2 was used with $\kappa = 0.3$.

ENVELOPE MODELING USING FINITE DIFFERENCES

Elastic FD synthetic seismograms were generated using the 2D CPU-based elastic wavefield modeling code *ewefd2d_omp* freely available through the Madagascar project (Fomel, 2016). The solver uses a second-order temporal and fourth-order spatial accuracy stentil. We performed twenty FD simulations with different heterogeneous velocities having the same statistical properties. We used a grid size of $dx = 0.025$ m with a time step of $dt = 1 \times 10^{-6}$ s, and domain size of 250 m x 250 m, resulting in 10^8 grid cells. For comparison with RTT MS envelope, each FD 2 components trace is squared and summed. The final FD MS envelope is obtained by stacking over all simulations corresponding to different random field realizations.

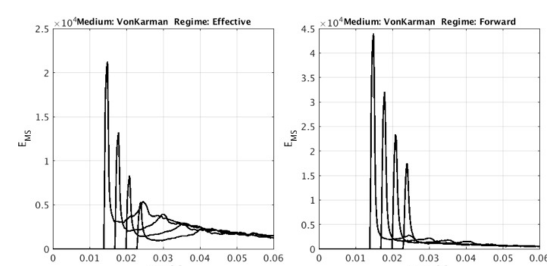

Figure 4: MS envelopes from MC simulations as a function of source detector distances for a von Karman medium, where $ak_s \sim 3.1$ (left) and $ak_s \sim 31$ (right). The offsets shown are: 50 m, 60 m, 70 m and 80 m.

RESULTS

In figures 4 and 5 show we compare the MS envelopes obtained from MC simulations and FD for both effective and forward scattering regimes. In both cases there is a good overall match between both methods for the P and S coda, although, there is significant differences at the peak of the P-wave arrival. We are currently investigating the causes of this mismatch, which we hypothesize is related to the short distance between source and receiver.

Figure 4 show a significant amount of S-wave energy arriving in the effective scattering regime ($ak_s \gg 1$) that is not present in the forward regime ($ak_s \sim 1$), even when the source only generates P-waves. This is the result of phase conversion on the path between the source and receiver. From figure 2 we note that in the effective scattering regime ($ak_s \sim 1$) the scattering coefficient g^0_{PS} is much larger than g^0_{SP}, meaning that there is larger probabilities of P-to-S conversion than S-to-P. Once P-to-S conversion occurs, it is less likely that S-to-P will occur. The P-to-S conversion occurs near the source, since the S-wave energy is concentrated at the S-wave arrival time.

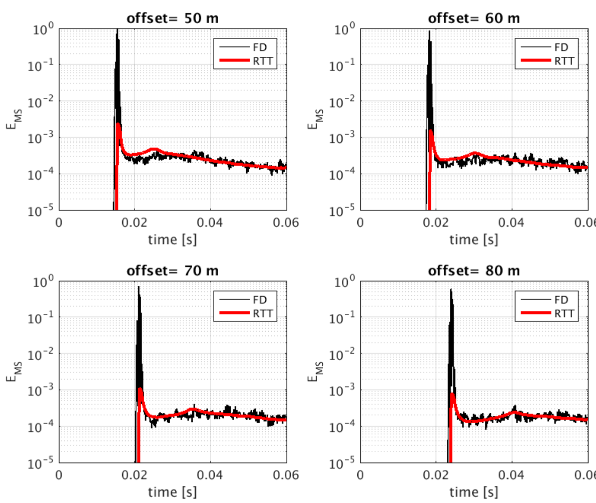

Figure 5: Normalized MS envelopes as a function of the source detector distance for a von Karman medium for $ak_s = 3.1$.

Apart from the balistic P-wave amplitude mismatch, the Monte Carlo simulation reproduces well the coda decay observed in the FD data. Further analysis is ongoing in order to determine which cases would result in a larger mismatch in the coda decay.

We measured the CPU time required to compute the MS envelope for both methods as a function of the domain size (figure 7) and found that the MC simulations is much faster than the FD, specially when $ak_s \sim 1$ since in this case we have large mean free paths (see table 2). Since each particle released from the source is independent of each other, we expect to further improve the MC simulation CPU time by distributing thousands of particles in several cluster nodes. With a fast MS envelope solver we expect to investigate in the future the sensitivity and trade offs of the mean square envelope to variations in the medium properties.

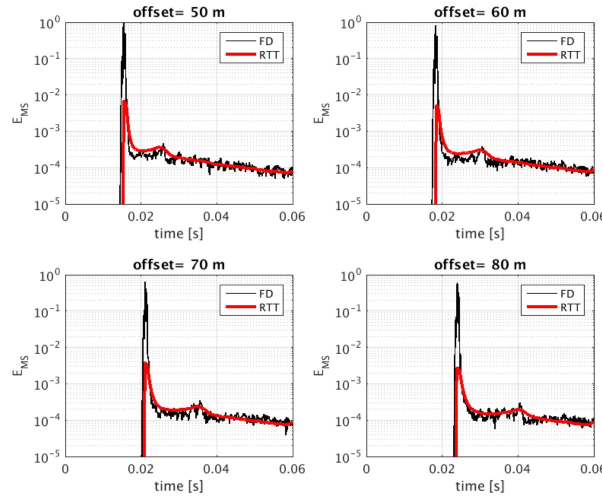

Figure 6: Same as figure 5 but for $ak_s = 31$.

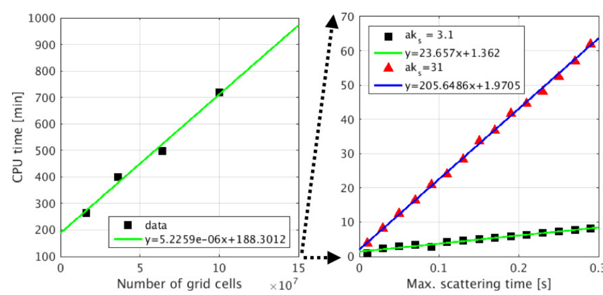

Figure 7: Approximate CPU time required to generate mean square envelopes for each scattering regime. The machine specifications are: x86-64 processor, 20 CPUs, 16 GB memory. For the Monte Carlo simulations it were used 10^4 particles, where the domain size is given by $V_s t_{max}$, where $t_{max} = 0.06$ is the maximum time that each particle is allowed to propagate. The finite differences parameters are described in the text. Note the difference in the CPU time scale.

CONCLUSIONS

We have shown that solving the radiative transfer equation using Monte Carlo simulations results in overall good agreement with synthetic envelopes generated using finite differences, except the peak amplitude of the onset P-wave. The MC simulations is computationally much faster than FD and therefore can be effectively used in investigating the inverse problem using, for example, a simple grid search. In the future we expect to use the MC method to characterize the random heterogeneities associated, for example, with fracture reservoirs.

ACKNOWLEDGMENTS

The authors would like to thank the founding members of the MIT Earth Resources Laboratory Consortium.

REFERENCES

Aki, K., and B. Chouet, 1975, Origin of Coda Waves - Source, Attenuation, and Scattering Effects: Journal of Geophysical Research, **80**, 3322–3342.

Chandrasekhar, S., 1950, Radiative transfer: Oxford, Clarendon Press, 1950. The International series of monographs on physics.

Daley, T. M., R. D. Solbau, J. B. Ajo-Franklin, and S. M. Benson, 2007, Continuous active-source seismic monitoring of CO2 injection in a brine aquifer: Geophysics, **72**, A57–A61.

Fomel, S., 2016, Madagascar web portal: http://www.ahay.org/RSF/sfewefd2d_omp.html (accessed 10 March 2016).

Gaebler, P., T. Eulenfeld, and U. Wegler, 2015, Seismic scattering and absorption parameters in the W-Bohemia/Vogtland region from elastic and acoustic radiative transfer theory: Geophysical Journal International, **203**, 1471–1481.

Klimes, L., 2002, Correlation functions of random media: Pure and Applied Geophysics, **159**, 1811–1831.

Paasschens, J. C. J., 1997, Solution of the time-dependent Boltzmann equation: Physical Review E, **56**, 1135–1141.

Przybilla, J., and M. Korn, 2008, Monte Carlo simulation of radiative energy transfer in continuous elastic random media - three-component envelopes and numerical validation: Geophysical Journal International, **173**, 566–576.

Przybilla, J., M. Korn, and U. Wegler, 2006, Radiative transfer of elastic waves versus finite difference simulations in two-dimensional random media: Journal of Geophysical Research-Solid Earth, **111**, B04305.

Przybilla, J., U. Wegler, and M. Korn, 2009, Estimation of crustal scattering parameters with elastic radiative transfer theory: Geophysical Journal International, **178**, 1105–1111.

Ryzhik, L., G. Papanicolaou, and J. Keller, 1996, Transport equations for elastic and other waves in random media: Wave Motion, **24**, 327–370.

Sato, H., M. C. Fehler, and T. Maeda, 2012, Seismic wave propagation and scattering in the heterogeneous earth: Berlin ; New York : Springer, c2012.

Shearer, P. M., and P. S. Earle, 2004, The global short-period wavefield modelled with a Monte Carlo seismic phonon method: Geophysical Journal International, **158**, 1103–1117.

Wegler, U., M. Korn, and J. Przybilla, 2006, Modeling Full Seismogram Envelopes Using Radiative Transfer Theory with Born Scattering Coefficients: pure and applied geophysics, **163**, 503–531.

Wu, R., Z. Xu, and X. Li, 1994, Heterogeneity Spectrum and Scale-Anisotropy in the Upper Crust Revealed: Geophysical Research Letters, **21**, 911–914.

Wu, R.-S., 1985, Multiple scattering and energy transfer of seismic waves separation of scattering effect from intrinsic attenuation I. Theoretical modelling: Geophysical Journal of the Royal Astronomical Society, **82**, 57–80.

Zeng, Y., 1993, Theory of Scattered P-Wave and S-Wave Energy in a Random Isotropic Scattering Medium: Bulletin of the Seismological Society of America, **83**, 1264–1276.

Zeng, Y., F. Su, and K. Aki, 1991, Scattering Wave Energy Propagation in a Random Isotropic Scattering Medium .1. Theory: Journal of Geophysical Research-Solid Earth and Planets, **96**, 607–619.